CHALMERS
UNIVERSITY OF TECHNOLOGY

Controlled release through inorganic/organic hybrid gels

Master's thesis within the Materials Engineering Program

Hanzhu Zhang

Controlled release through inorganic/organic hybrid gels

60 hp Master's thesis within the Materials Engineering Programme
Course code: KBTX60

by Hanzhu Zhang

Department of Chemical and Biological Engineering
Division of Applied Chemistry, Chalmers University of Technology
Gothenburg, Sweden, August, 2014

Cover image:

Liquid permeability and PNIPAM microgel particle size as a function of temperature in a composite gel made of 22 wt% colloidal silica and 1.4 wt% PNIPAM microgels. The two inserted images illustrate the rheological behaviour of the gel/dispersion at 25°C and 40°C, respectively.

Department of Chemical and Biological Engineering

Chalmers University of Technology

SE-412 96, Gothenburg, Sweden

Telephone +46 (0)31-772 1000

Abstract

This thesis explores the area of sol-gel formulation and characterization of a new composite gel material consisting of a colloidal silica matrix with poly(N-isopropylacrylamide) microgels dispersed within the matrix. The microgels shrink dramatically in size when heated above 32°C and reversibly re-swell when cooled below this temperature. The size changes in the microgels are used to control liquid flow through gels as the microgel form an open and closed porous network through the silica matrix in their contracted and swelled state, respectively. Such responsive gels can be used as temperature responsive liquid flow switches for application in for example everyday consumer products, clinical drug delivery or advanced nanotechnology devices.

Both lyophilisation and ultracentrifugation were tried as methods for concentrating the microgel dispersions and the latter was found to be the best as these microgels were easier to disperse. Microgel concentration between 0 and 1.8wt% was found to produce gels stable to temperature cycling and gels with 1.6 wt% polymer produced the maximum change (113%) in flow speed in response to cycling. In contrast, the relative diffusion ($D_{composite}/D_{silica\ only}$) did not change in response to temperature, and hence the gels can be used to vary pressure induced liquid flow but not liquid diffusion over the gels.

Table of Contents

1. Introduction

1.1. What is controlled release and why is important?

In modern society, different kinds of substances, such as drugs, fertilizers and pesticides need to be released in a special way to provide their function. Often the use of the releasing substance is more efficient if it is delivered to the target at the right time, place and in the right amount. Therefore much research has been focused on realising such systems during the last decades [1].

To control the delivery of a drug, several different mechanisms can be used. A releasing substance, for example a drug, can be mixed with a polymeric matrix and the chemical and physical properties of this matrix can be controlled to design the release. Often the release is affected by surrounding environment factors such as pH [2], salt concentration [3], and fat content [4]. Compared to passive release that continuously release a substances with little possibility of affecting the release, for example, when a pill has been swallowed, on-demand controlled release systems have been explored to improve the temporal and spatial presentation of a drug in human's body. Such systems offer many advantages including the use of controlled feedback mechanisms to deliver the drug only when needed. For example, a diabetic patient can with such a system trigger insulin release in an implanted device after detecting too high levels of glucose in the blood. Implanted systems can be used for site specific drug delivery that makes it possible to have a higher drug concentration for more efficient treatment, but systemically lower concentration, which reduces the risk of unwanted drug side effects [5].

1.2. Project plan

1.2.1. Purpose

In nanotechnology applications both in chemistry and biology there is a need for soft gel materials that can be designed to perform advanced control release functions as a response to environmental factors or triggered signals. These materials function as valves that turn on and off the release of diffusing or flowing substances [6, 7]. As these materials often consist of mainly water there is an additional need for a better understand the water dynamics within such materials.

1.2.2. Goal

The goal was to formulate a new type composite gel consisting of a colloidal silica matrix with poly(N-isopropylacrylamide) (PNIPAM) microgels. The work aimed to characterize the gels mechanical properties and its ability to affect liquid diffusion and pressure induced flow, or osmotic gradient induced flow, as a function of variations in temperature. It was hypothesized that temperature induced shrinking and swelling of the embedded microgels could be used to control the water diffusion and flow through the gels.

2. Background

2.1. Controlled release

2.1.1. Passive release

Passive release from a material is a type of controlled release that cannot be varied actively. Often the substance diffuses out from a matrix material in which the drug has fixed solubility. The matrix can also have a certain pore structure. Both the solubility and pore structure of the material results in a specific diffusive resistance to the releasing substance that gives a specific drug release profile. In some cases the matrix is degradable and as it is broken down new substance can be released. The release of encapsulated or tethered drugs can occur during surface erosion or bulk degradation of the polymer backbone [8, 9]. Such release is for example used for perfumes, drug and biocides in boat hull paint [10].

2.1.2. Active release

Active release systems can be trigged by a substance in the surrounding medium such as chemical substance [11], pH [12], temperature [13], osmotic pressure [14] or a signal as will be described below under 'on-demand drug release'.

2.1.3. On-demand active controlled release

On-demand active controlled release is a type of active controlled release in which the user induces the release of a substance. The release can for an implant be remotely triggered by a signal, for example ultrasound [15], magnetism [16], radiosignals [17, 18] or light [19].

2.1.4. Temperature responsive release

The advantage of temperature controlled release is the ability to release drug by local heating and the more direct and accurate control of the release rate. Thermoresponsive polymers have been explored to achieve such release [20]. In 2003, Chu and colleagues prepared such a system consisting of a porous membrane that has grafted PNIPAM polymer on the walls of the pores. This made it possible to change the permeability over the membrane by varying the temperature [21]. Figure 1 shows how Suzuki and colleagues adjusted the flow rate in a microfluidic channel using a thermosensitive polymer [22].
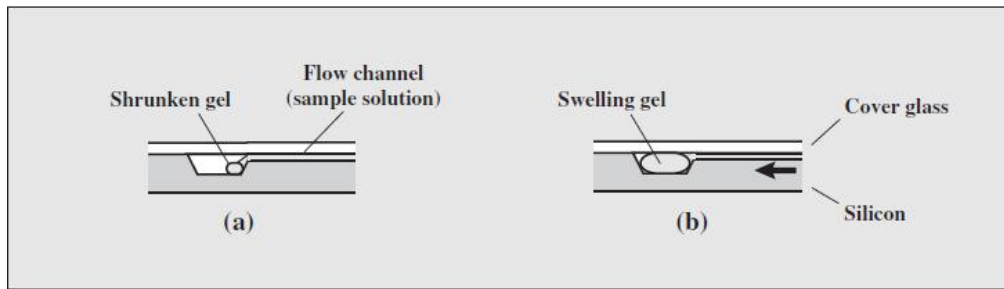
Figure 1 On-demand control of liquid flow through a channel using a thermosensitive polymer (with permission from SAGE, ref [22], copyright 2006).

2.2. Mass transport

There are two mechanisms of mass transport in gels, i.e. diffusion and flow. Diffusion is governed by the Brownian motion of the molecules. Molecules migrate from regions of high substance concentration to low concentration regions. Diffusion as a process is generally very slow and often is unobservable by the naked eye [23]. The second mechanism of mass transport is flow. Compared to diffusion flow is usually caused by a pressure gradients, but sometimes also by concentration gradients. Flow is a faster process and it requires bulk motion of many molecules in contrast to diffusion.

2.2.1. Diffusion

In 1855, Physiologist Adolf Fick described what was later named Fick's Law, which is commonly used to describe the diffusion process:

$$\mathbf{J} = -\mathbf{D}\frac{\partial \emptyset}{\partial x} \qquad \text{[Equation 1]}$$

Where J is the diffusion flux, with the dimension is mol/m^2s;

D is the diffusion coefficient has the dimension of m^2/s;

Φ is the concentration with dimension mol/m^3;

x is the length in meters. [24]

2.2.2. Flow

Darcy's law is used to describe flow of a fluid through a porous medium. The equation was formulated by Henry Darcy in 1856 when he was studying water flowing through sand filters in public water supplies [25]. The original equation is:

$$\mathbf{v} = -\mathbf{K}\frac{dh}{dl} \qquad \text{[Equation 2]}$$

Where v is flow speed, K is hydraulic conductivity, which describes the movement of a fluid through a geological material.

Darcy's law can also be written as,

$$\mathbf{v} = -\frac{k\rho g}{\mu}\frac{dh}{dl}\mathbf{A} \qquad \text{[Equation 3]}$$

Where A is the cross sectional area of the material (gel thickness) and µ is the dynamic viscosity of the fluid.

$k=Cd^2$ is the intrinsic permeability (L^2), where d is the diameter of the particles, C is constant which depends on the shape of the particle openings [25].

2.3. Colloidal stability

A colloidal particle have at least one dimension in the size range of 1 nm to 1 µm. Colloidal systems have large surface area per volume material, a property that in many ways define the characteristics of the system [26].

A stable colloidal dispersion consists of a liquid with dispersed particles that do not aggregate or sediment. The particles are usually stabilised by surface charges, or steric interaction coming from adsorbed or grafted polymer strands [27]. A high surface charge will result in high repulsive forces between particles of the same charge, which could increase the stability of colloidal system. The stability is also affected by factors in the surrounding medium, such as particle concentration, ionic strength and pH [28, 29]. The particle size also affect the colloidal stability and each system have an ideal particle size range for maximum colloidal stability [30].

2.4. DLVO theory

The Derjaguin-Landau-Verwey-Overbeek (DLVO) theory describes the interparticle interactions in colloidal suspension. It describes colloidal stability in terms of a balance

between two types of forces: attractive van der Waals forces (V_A) and repulsive electrical double-layer forces (V_R). The net interaction forces (V_T) is given by:

$$\mathbf{V_T = V_A + V_R} \qquad \text{[Equation 4]}$$

Figure 2 illustrate how the attractive forces decays with a power function while the repulsive forces decreases exponentially with increasing distance (x) between two particles [31]. The combination (blue curve) of both forces decides if the system is colloidally stable or not.
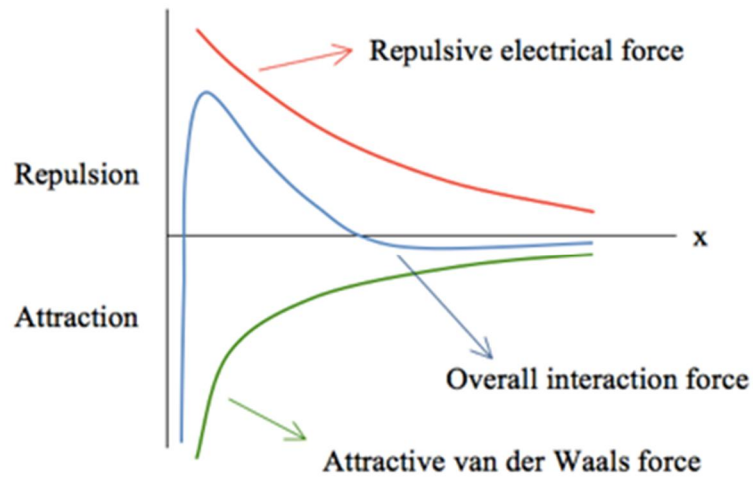
Figure 2 Schematic of interaction forces in a colloidal system.

The repulsive electrical force in colloidal system can be characterized by the zeta potential. Zeta potential is the electrical potential of the outmost plane of the double layer, which is called 'slipping plane'.

As shown in Figure 3, the electrical double layer consist an ion cloud next to a charged surface, that has a higher concentration of ions compared to the bulk liquid [32]. The electrical double layer consists of two layers (Figure 3). The layer closest to the surface is called the Stern layer and it consists of adsorbed ions that are oppositely charged compared to the surface. Outside of the stern layer, there is a diffuse layer that consists of ions of alternating charge but with more ions of opposite charge compared to the surface, close to the surface [33]. In colloidal systems, the repulsive electrostatic force due to double layer structure often plays a dominant role [34].
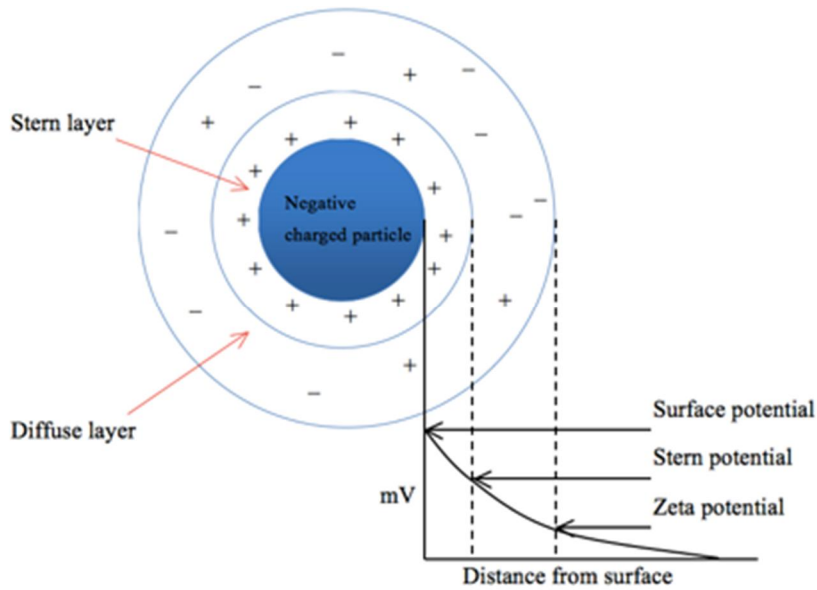
Figure 3 Schematic of the of electrical double layer around a negatively charged particle (with permission from Royal Society of Chemistry, ref [35], copyright 2013).

2.4.1. Gelation, flocculation and sedimentation

Gelation, flocculation and sedimentation often results from particle aggregation. They are often manifested by an increase in turbidity or a change in colour. Sol gelation is often described as a process that starts with particle aggregation of individual particles in the sol. As the particle aggregates grow the sol viscosity increases and finally gelation or flocculation occurs. The gel is a large aggregate particle network that spans the whole volume of the sample, effectively binding the liquid that permeates the network structure. If there are not enough of particles to span the whole volume, the aggregates will form loose flocculates that cause phase separation or denser sediments that settle to the bottom of the sample [26]. Figure 4 illustrates the structure of a sol, gel and flocculate.
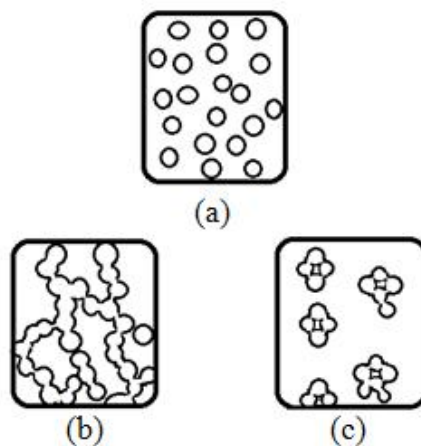
Figure 4 Descriptions of (a) sol, (b) gel, (c) flocculation or sedimentation.

7

2.4.2. Ostwald ripening

Ostwald ripening, also known as coarsening, can occur in for example small particle dispersions [36]. This phenomenon is often explained in two different ways.

The first explanation says that convex surfaces are more soluble than concave surfaces. When two spherical particles are in contact with each other the concave connecting neck between them begins to grow as material is transported from the convex surfaces of the particles [37].

The second explanation states that the large surface energy of the small particles causes Ostwald ripening. As the system strives to minimize the interfacial area and the surface energy, Ostwald ripening will occur as the total energy of the system will be decreased when the surface area is reduced [38].

2.5. Colloidal silica

2.5.1. Silica

Silica is a silicon oxide that can be found in nature as sand or quartz. Silica makes up about 12% of the weight of earth's crust, in the form of amorphous and crystalline species. The structure of silica is illustrated in Figure 5. The silicon atoms are located at each centre of a tetrahedron, with four oxygen atoms occupying the vertexes.
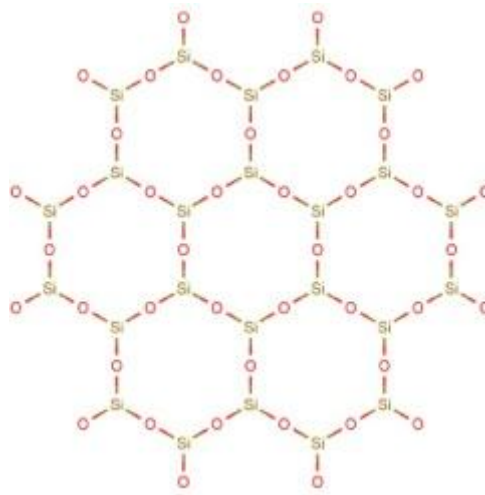
Figure 5 Silica structure.

2.5.2. Colloidal silica sols

A colloidal silica sols consist of nanometer sized silica particles dispersed in a liquid. The surface of the silica particles is most often covered by silanol groups [39]. When the particles aggregate, siloxane bonds are formed according to the following reaction:

$$Si\text{-}OH + HO\text{-}Si \rightarrow Si\text{-}O\text{-}Si + H_2O \quad (10)$$
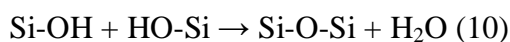
Just as for other types of charge stabilized sols, silica sol stability often depend on the sol pH and ionic strength [40]. Figure 6 illustrates how the colloidal stability is affected by pH and salt concentration. The longer the gel time, the more stable is the colloidal system. Figure 6 shows that a minimum in the stability for silica sols can be found around pH 6 while regions of higher stability is found at high pH or in the metastable region around pH 2. If the pH is too basic the silica can dissolve.
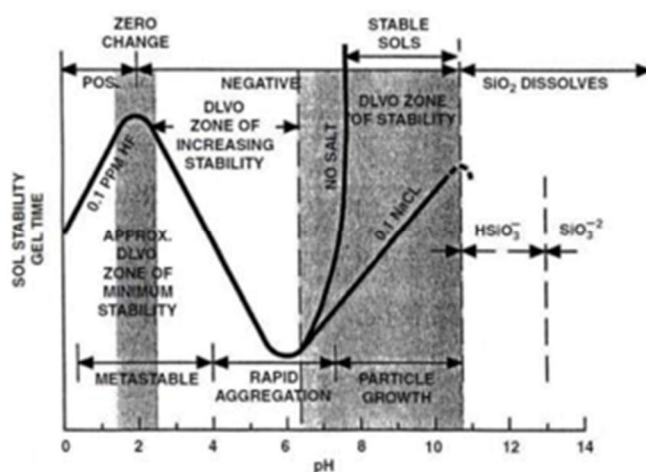
Figure 6 The effect of pH on colloidal silica stability (with permission from John Wiley & Sons, ref[40], copyright 1979).

2.6. PNIPAM

2.6.1. Chemical formula and chemical groups

PNIPAM (Poly(N-isopropylacrylamide)) is a polymer well known for its response to temperature. As shown in Figure 7, PNIPAM has both hydrophilic (amide) and hydrophobic (isopropyl) groups. This molecular structure experiences a configuration change as response to temperature variations.
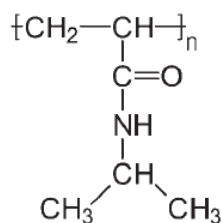
Figure 7 Chemical structure of PNIPAM

Because of the thermal responsiveness, PNIPAM is widely used in biotechnology and medicine in a wide range of applications. It has for example been used in coatings for absorption and release of proteins from surfaces [41]. Also, PNIPAM microgels have been used for removing heavy metal ions from waste water [42].

2.6.2. Thermal response of microgels

The LCST that is also known as the Lower Critical Solution Temperature, is the highest temperature at which the polymer is well miscible in water. Above this temperature the polymer dispersion gets cloudy. For PNIPAM, the LCST is around 32°C.

Below the LCST, the amide groups will extend into the aqueous environment to participate in hydrogen bonding with water molecules. In this configuration the hydrophobic isopropyl groups bend inwards which results in hydrogen bonding with the polar amide groups, lowering the surface energy. In this state PNIPAM chains takes a random-coil configuration.

Above the LCST, the hydrophobic isopropyl groups orient outward to maximize hydrogen bonding within the polymer. In this state the polymer have compact globular configuration [43]. It is however wrong to describe the PNIPAM as hydrophobic above its LCST. Even in this state the water content of the PNIPAM is around 20-50% [44-46]. Instead PNIPAM has both hydrophilic and hydrophobic properties above LCST but the hydrophobic domains dominate the dispersed polymers phase behaviour [7].

2.6.3. PNIPAM microgel surface charge

Pure PNIPAM microgels in distilled water have been found to have a negative potential of -18mV [47]. The negative charge of PNIPAM microgels originates from sulphate groups that are introduced during the PNIPAM synthesis when using the reaction initiator ammonium persulfate.

In solution at low pH, the sulphate groups are easily hydrolysed to form uncharged hydroxyl groups.

$$R-OSO_3^- + H_2O \xrightarrow{H^+} R-OH + HSO_4^-$$
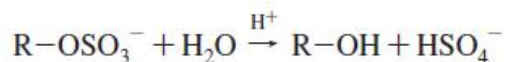
2.7. Material mechanism for controlled release

When the temperature exceeds the LCST of the PNIPAM microgels, they will contract and expel water in the process. It is theorized that at high enough concentration of polymer most microgels will be in contact with each other. When the microgels then shrink a liquid filled pore space will be formed between the contracted PNIPAM microgel and the silica matrix. This pore space will form a connected network through the gel where a solvent or solute can diffuse or flow.

3. Experimental methods

3.1. Materials

A colloidal silica sol (22.72 vol% silica, BINDZIL 50/80) was kindly provided by Akzonobel Pulp and Performance Chemicals, Sweden. The density of the silica particles was 2.2 g/cm^3 [48]. Methylene blue, Sodium chloride, N-isopropylacrylamide (NIPAM), N,N-methylenebisacrylamide (MBA), N-isopropylmethacrylamide (NIPMAM), acrylamide (AAm) and ammonium persulfate were purchased from Sigma-Aldrich.

3.2. Silica gel salt concentration optimization

A phase diagram was made where the NaCl concentration was varied to find the concentration that was needed in order to get stable silica gels. The goal was to find the minimum salt concentration needed to produce mechanically stable gels that gelled in relative short time for quick sample preparation. With a low salt concentration, possible disturbance on the PNIPAM temperature response and salt crystallisation within the samples could be avoided. Gelation and sample mechanical integrity was assessed using an inverted tube test.

3.3. Composite gel formulation

The inverted tube test was performed by inverting the tube and gently shaking it. Samples were prepared in 1.5 ml Eppendorf tubes by mixing a 2.5 M NaCl solution, water and silica sol, followed by a few seconds of vortexing. The sample solution was then pipetted into glass vial, NMR tubes or the flow columns that were sealed to let the sols to gel during a few days. A high silica concentration was desired to minimize the water leakage through the silica matrix of the gels instead of the pores formed by the contracting PNIPAM microgels. Therefore the silica concentration for all samples was set to 10 vol% (equivalent to 22 wt%).

The following classification was made of the phase behaviour when the sample tube was inverted upside down. If the sample was flowing, it was a 'liquid'. Moreover, if it flowed only after a gentle shake it was defined as a 'liquid-gel'. Finally, if the sample did not flow it was a 'gel'.

An additional benefit with the silica matrix is that it hinders phase separation of the silica and PNIPAM particles over time.

3.4. PNIPAM synthesize

The synthesis of the PNIPAM microgels was done by polymerization of N-isopropylacrylamide (NIPAM) as previously reported in literature [49]. Typically, 1.35g N-isopropylacrylamide (NIPAM) and 0.08g methylenebisacrylamide (MBA) were dissolved in 150ml Milli-Q water (from here on referred to as water) and heated to 70°C under magnetic stirring and purged with nitrogen gas for 30 minutes in a 500 ml round bottom three-neck flask under reflux. After that, 0.1g ammonium persulfate was dissolved in 5ml water and injected dropwise into the flask. The reaction continued under stirring for 4 hours and the reaction mixture was then cooled to room temperature. The reaction mixture was then dialyzed against deionized water until there was no change in conductivity to get rid of unreacted salt and monomers. Two different methods were successfully used to concentrate the dialysed PNIPAM solution. Lyophilisation was the first method [16]. The second method employed ultracentrifugation of the dialysed solution at 14000 RPM for 2.5 hours. A part of the sediment was used to determine the polymer dry weight concentration and the rest was redispered to form the different silica-PNIPAM gels.

A batch of microgels made from a PNIPAM-co-polymer with a LCST around 42°C was synthesized by the method used by Hoare and colleagues [16]. The polymerization process is

similar with the PNIPAM microgel synthesis, but with 0.4685g NIPAM, 0.8726g NIPMAM, 0.0589g AAm and 0.08g MBA being used as monomers and cross linker.

3.5. PNIPAM microgel characterization

The thermoresponsiveness of the microgels was checked at room temperature and at 40°C by imaging the sample transparency/opaqueness and by observing the mechanical properties of PNIPAM pellet in 1.5 ml glass vials. PNIPAM suspension was observed by optical microscopy (DP12 Microscope Digital Camera System, OLYMPUS, Japan). A melting point system (MP70 Melting Point System, METTLER TOLEDO, USA) was used to monitor the appearance change of PNIPAM when varying temperature. In addition, the size distribution of microgel particles with different LCST (32°C, 42°C respectively) was measured at different temperatures by Dynamic Light Scattering (Zetasizer Nano ZS, Malvern Instruments, UK). Before measurements, the sample was allowed to equilibrate in the instrument for about 20 minutes after each temperature change.

3.6. Flow measurement

The flow speeds of a 0.5M NaCl solution passing through the different samples was measured to find the liquid permeability of the gels. The measurement was performed at different temperatures: 25°C, 30°C, 32°C, 34°C and 39°C. The columns used to measure the flow speed were constructed as previously described [48], see Figure 8. In short, the bottom of a 5 mm in diameter glass NMR tube was removed forming a glass tube to which a 210 micron polyester mesh was glued to support the gel. The meshed end was sealed with Parafilm and the column was filled up with sample sol 30 mm from the mesh and then the other end was sealed with Parafilm. After letting the sample gel for a week, the Parafilm was removed and the column was fixed upright in a stand in a water bath (RTE-200P, NESLAB, Newington, GA, USA) filled with 90 mm of 0.5 M NaCl solution with the surface level in bath the at the same level as the top of the gel plugs in the columns. A magnetic stirrer ensured good mixing in the water bath. Columns were then filled with 90 mm of 0.5 M NaCl solution on top of the gel to create a pressure gradient over the gels. The position of the top of the salt solution was recorded over time by marking the column with a marker pen 2 times a day for at least 3 days. Before changing the temperature the column was refilled with salt solution and the rest of the procedure was then repeated as above.

The flow rate was calculated from the surface level change as a function of time, being close to linear for the first week in all samples. Darcy's law was then used to calculate the permeability.
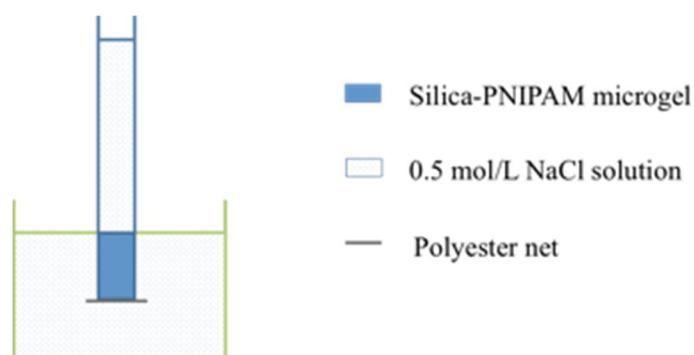
Figure 8 Experimental set-up for flow measurements.

3.7. Osmotic pressure diffusion measurements

In the osmotic diffusion measurement, methylene blue was used as the substance that would pass through the microgel. The set up was similar to the flow measurement, but the NaCl solution above the gel was replaced by 0.3ml of saturated methylene blue solution. The NaCl concentration in methylene blue solution and the receiver compartment was 0.5 M. Therefore the driving force of molecular movement was only osmotic pressure provided by the concentration gradient of methylene blue. The composite gels were prepared in the same way as for the flow measurements. The level in the receiver was kept the same with methylene blue solution, and the whole system was well sealed with parafilm.

During the measurement, samples with 0.6ml solution were taken out of the receiver compartment once per hour. The methylene blue concentration was characterized by Ultraviolet–Visible spectroscopy.
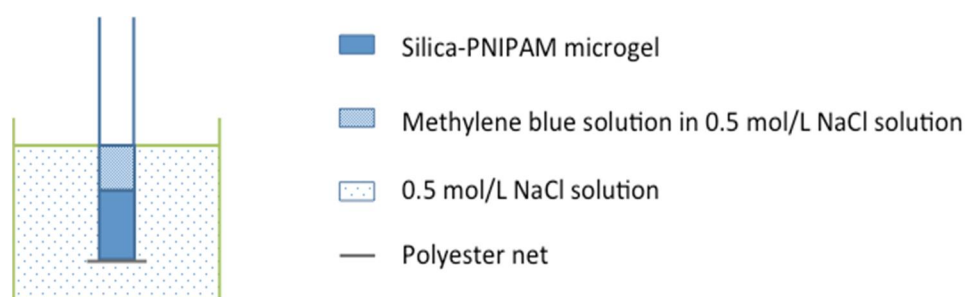
Figure 9 Designed system set-up for diffusion measurement.

3.8. NMR-diffusion measurements

NMR experiments were performed with a Bruker Avance 600 spectrometer (Bruker, Karlsruhe, Germany) with a diffusion probe with a maximum gradient strength of 1200 G/cm and with a 5 mm RF insert with 1H and 2H coils. All diffusion experiments were performed with $\Delta=500$ ms diffusion time, $\delta = 1$ ms gradient pulse length, and the gradient strength linearly ramped in 17 steps from 0 to 30.03 G/cm in the conventional stimulated-echo sequence. Relaxation delay to thermal equilibrium, D1, was set to 20 s and each experiment encompassed a collection of 1 acquisitions.

4. Results

4.1. Silica gelation time at different NaCl concentrations

The gelation of the silica sol in the presence of different salt concentrations was investigated with an inverted tube test. All samples contained 10 vol% silica and Table 1 show how changes in the NaCl concentration affected the gelation times. In short, increased NaCl concentration resulted in shorter gelation times.

NaCl concentration (M)	Bindzil 50/80
0.9	6 min
0.7	26min
0.5	1-1.5 hour
0.3	More than 1 day

Table 1 Gel time of Bindzil 50/80 with varied NaCl concentration.

As shown in Table 1 the gel time of the sample with 0.9 M NaCl was only 6 minutes. The gelling time increased sharply when salt concentration was slightly reduced. It took more than one day for samples with a NaCl concentration lower than 0.5 M. It was decided that a salt concentration of 0.5 M NaCl would be most suitable for the continued formulation of the silica-PNIPAM composites as that salt concentration offered a good compromise between and mechanical strength and gel time.

4.2. PNIPAM microgel characterization

4.2.1. Thermal response of PNIPAM
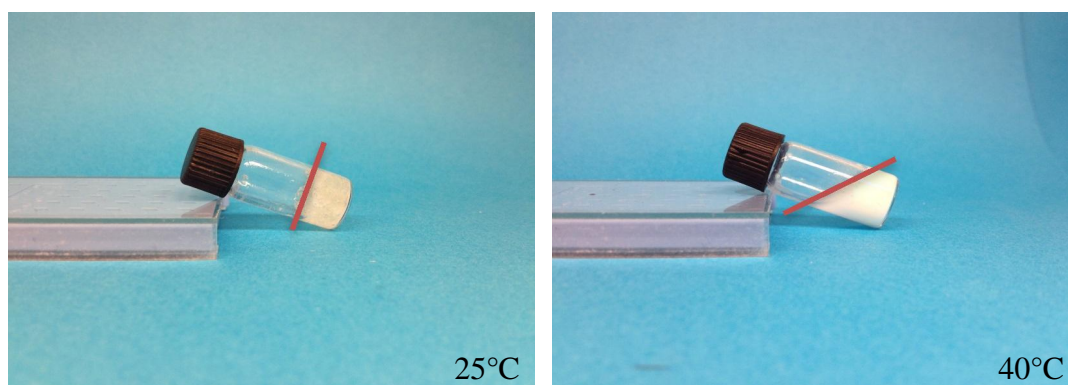
Figure 10 Thermal response of a 25 wt% PNIPAM gel sample (contains no silica or salt).

The sample shown in Figure 10 contained 25 wt% of PNIPAM. At room temperature, it was a semi-transparent gel. If the tube was tilted or inverted, it remained at the bottom and would not flow. After heating the sample to 40°C, the sample quickly became opaque. The sample also expelled water that formed the tilted liquid surface in Figure 10 (right).
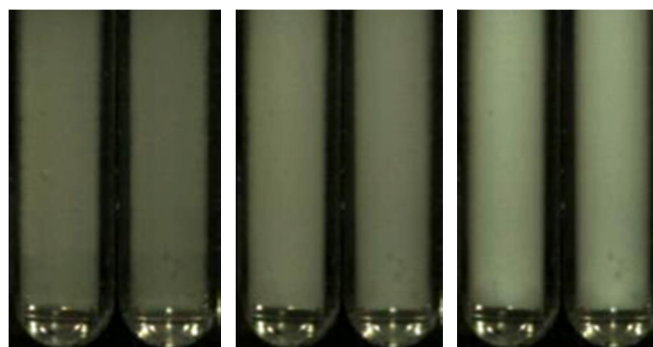
Figure 11 LCST observation of uncentrifuged PNIPAM suspension in glass capillaries. Temperatures were 27°C (left), 32°C (middle) and 39°C (right), respectively.

Two uncentrifuged PNIPAM suspension samples (dry weight around 0.7wt%) were put in the melting point testing apparatus. The instrument takes images of the PNIPAM dispersion filled capillaries as the samples were heated. The samples started to become more opaque close to 32°C, and grew even more opaque as the samples reached 39°C (Figure 11).

4.2.2. Optical microscopy of PNIPAM suspension
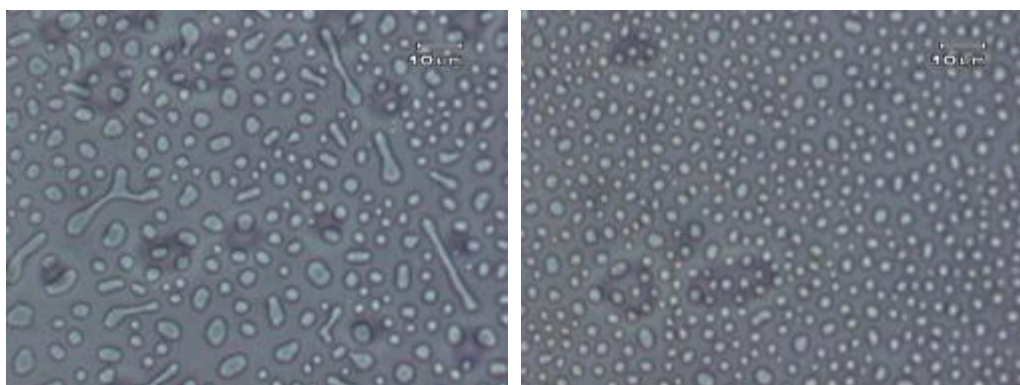
Figure 12 Microgels in small water droplets observed by light microscopy

Optical microscopy was performed to observe the microgels. A drop of uncentrifuged microgel solution with 0.61 wt% of PNIPAM was observed on a glass slide. The microgels was never observed directly. However, it was hypothesized that the drops left behind on the glass slide were partly dried out microgels, possibly with some extra water. Based on that hypothesis Figure 12 (left) shows microgels with extra water bridging between microgels. If the hypothesis is true, Figure 12 (right) illustrates that the microgels had an average size of around 3 µm. The diameter of the microgel particles was estimated by the software ImageJ after measurement of 90 particles. It is possible that the microgels were surrounded by a certain amount of water making this estimation larger than the real diameter of the microgels. Moreover, it is possible that the microgels were slightly compressed by the cover glass making the average diameter larger than the real size.

4.2.3. PNIPAM particle size measurement

The aim of particle size measurement was to do a statically relevant size estimation of the swelling and collapse of PNIPAM microgels.
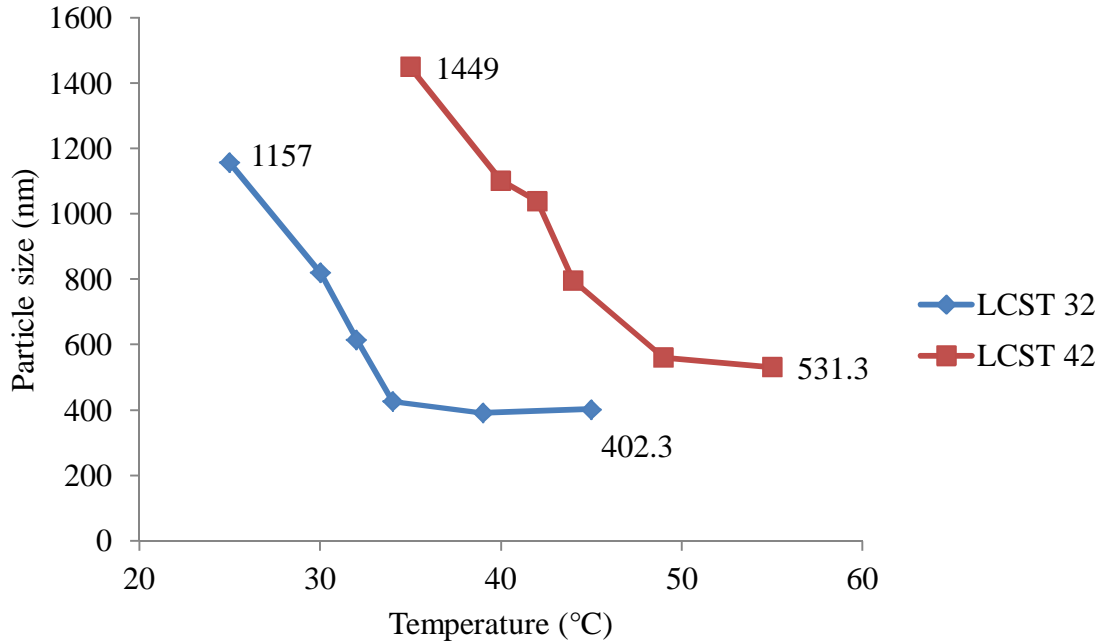
Figure 13 DLS measurement of PNIPAM (LCST 32) and PNIPAM-copolymer (LCST 42) microgel diameter at different temperatures.

Figure 13 shows the microgel size change as a function of temperature. For PNIPAM with 32°C as LCST, the diameter of PNIPAM particles was round 1150 nm at 25°C, which was the lowest temperature tested. As expected, the microgel diameter decreased as the temperature exceeded and passed the LCST of PNIPAM. As the temperature was increased, the size of particles decreased dramatically reaching around 400 nm at 45°C, which was approximately 30% of the diameter at 25°C. The results were smaller than that found from the optical microscopy images in Figure 12, which confirms that the microscopy over-estimate the microgel size.

The PNIPAM-co-polymer microgels with a LCST of 42°C were slightly larger having a diameter of around 1450 nm at 32°C and around 530 nm at 55°C. Both of them had about 2/3 reduction of the diameter when the temperature was increased 20 degrees around their LCST.

4.3. Sample formulation

Different PNIPAM microgel concentrations in the silica-PNIPAM gels were investigated to find the optimum concentration for large changes in the mass transport properties, while at the same time maintaining the structural integrity of the gels. The gels was temperature cycled, and in this process the size changes in the microgels are likely to cause significant mechanical stress on the gel particle network.

4.3.1. Sample formulation - silica with lyophilised PNIPAM

After polymerization of PNIPAM, the polymer suspension was first lyophilized to get dry polymer. It was frozen overnight in a refrigerator before lyophilisation.
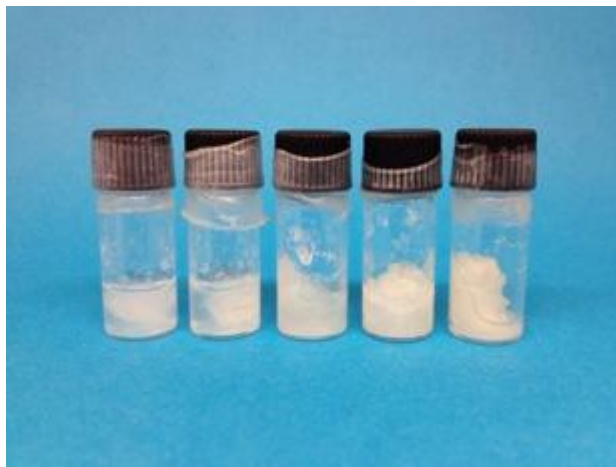
Figure 14 10 vol% colloidal silica mixed with different amounts of lyophilized PNIPAM. The PNIPAM concentrations from right to left were: 10wt%, 15wt%, 20wt%, 25wt% and 30wt%.

As seen in Figure 14, the lyophilized PNIPAM was hard to disperse well in the silica sol. The mixing is so incomplete that the dispersion of the lyophilized PNIPAM was judged to be unsuccessful. Therefore another method of concentrating the PNIPAM was explored as presented just below.

4.3.2. Sample formulation - silica with centrifuged PNIPAM

From here on the concentration of silica in the gels is always 10 vol% and the NaCl concentration is 0.5M. First the dialysed PNIPAM dispersion was ultracentrifuged to obtain a PNIPAM microgel sediment. The polymer concentration in the centrifuged PNIPAM pellet was determined to be 6.08 wt% which meant that the highest concentration of PNIPAM achievable (after adding salt and silica sol) would be 3.27wt%. Such a sample was successfully mixed and it was allowed to gel for 1 week. When the gel was heated up to 40° the whole gel broke as the gel shrank. For the following experiments lower polymer concentrations were investigated to find a PNIPAM concentration range in which the gels remained structurally intact after temperature cycling.

A series of samples was made with colloidal silica and a PNIPAM concentration between 0 to 2.1 wt%. The PNIPAM microgels were easy to disperse well for all samples.

PNIPAM concentration	25°C	40°C
0 wt%		
1.0 wt%		
1.4 wt%		
1.6 wt%		
1.8 wt%		
2.1 wt%		

Figure 15 Structural integrity of silica-PNIPAM gels at varied PNIPAM concentrations and temperatures.

Figure 15 show that all samples have a similar appearance at 25°C. Even at 40°C there were no large differences in appearance between samples with PNIPAM concentration from 0 to 1.6 wt% as they all remained structurally intact after temperature cycling. However, some expelled water was found on the top of the gel with 1.8 wt% PNIPAM. About 10% of that gel sample volume consisted of this expelled water. After heating the sample with 2.1 wt% PNIPAM, a small crack formed on the top of gel when the tube was slightly shaken. Moreover, samples with a PNIPAM concentration higher than 2.1 wt% (data not shown) experienced structural failure, breaking up into pieces and sedimenting when heated to 40°C. Therefore mass transport measurements were only done with samples with a PNIPAM concentration up to 1.8 wt%.

4.4. Silica-PNIPAM composite gel liquid permeability

Figure 16 illustrates how the liquid permeability of the gels changed when varying for the PNIPAM concentration and temperature. For the pure silica gel, the liquid permeability was roughly 1 mD. Compared to the pure silica sample, the permeability at 1, 1.4, 1.6 and 1.8 wt% PNIPAM concentration increased 30%, 57%, 113% and 103%, respectively. The permeability of the pure silica sample also experienced a small increase when the temperature was increased. As the temperature was increased in the samples, the largest permeability increase occurred below the 32°C - LCST temperature of PNIPAM. In the pure silica gels however, the small permeability increase appeared to be almost linearly dependant on the temperature. The samples with 1.4 and 1.6 wt% PNIPAM had the largest absolute change in permeability.
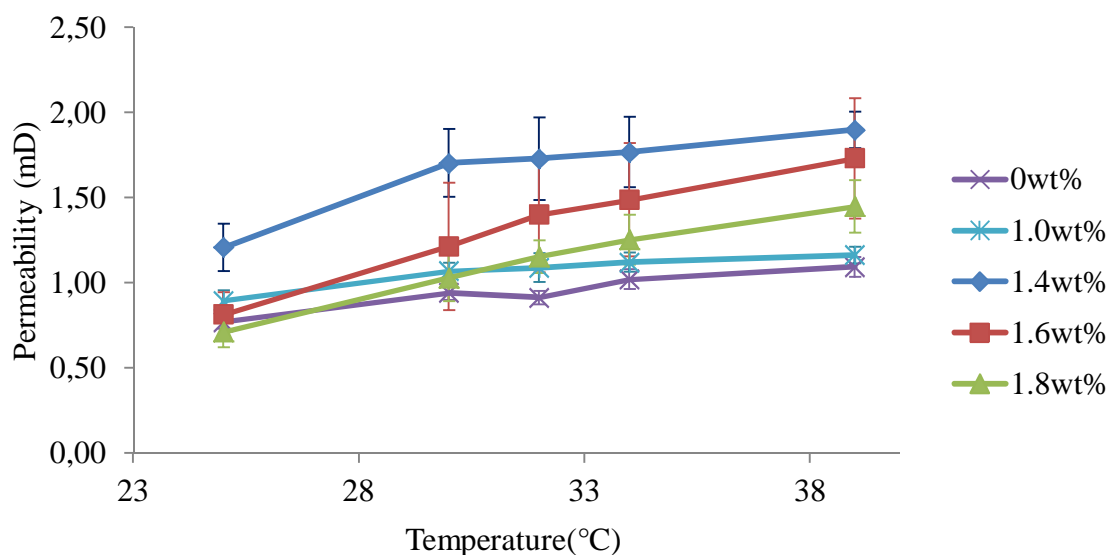

Figure 16 Comparison between liquid permeability (flow measurements) and microgel size (DLS data) as a function of temperature.

The gels with 1.4 wt% PNIPAM showed the highest permeability among all the samples. Below in Figure 17 the microgel size and liquid permeability as a function of temperature is presented.
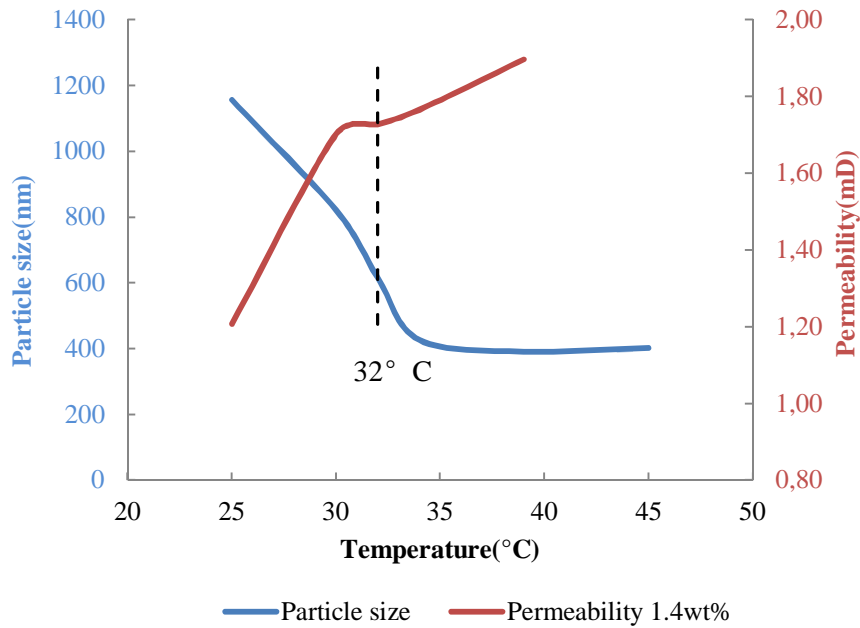
Figure 17 Comparison between liquid permeability (flow measurements) and microgel size (DLS data) as a function of temperature.

4.5. Effect of temperature cycling on gel permeability

During the temperature cycling the temperature of the gels was varied back and forth between 25 and 39°C to investigate if the mass transport changes were reproducible for many temperature cycles. Figure 18 illustrates that a change from 25 to 30°C resulted in a sharp permeability increase, but between 30 and 39°C the permeability increased less. The same figure also shows that the permeability experienced hysteresis, that is the gel permeability was not the same when the temperatures was increased compared to when it was decreased.
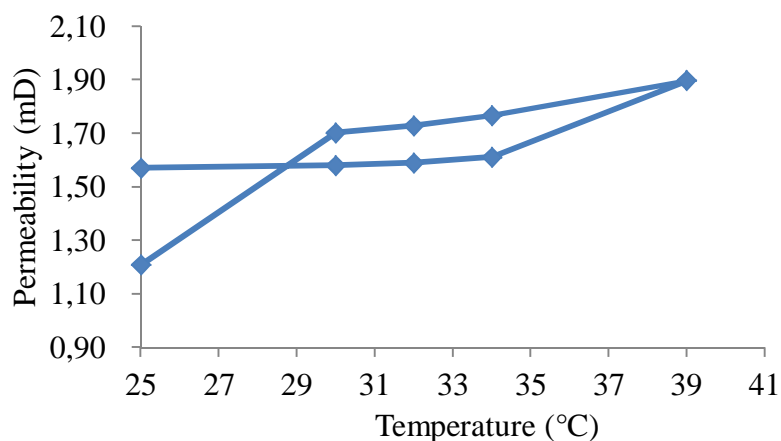
Figure 18 Liquid permeability of a gel with 1.4 wt% PNIPAM as a function of increasing and decreasing temperature. The first data point has a permeability of 1.21 mD

The permeability increased between 30 to 119% when the temperature was increased from 25 to 39°C, depending on PNIPAM concentration. Figure 19 proves that the silica-PNIPAM composite gels can vary their permeability reversibly when the temperature is cycled. In Figure 19 (b), the permeability ratio P/P_0 was calculated by dividing the measured permeability by the permeability at 25°C before the first temperature change. The biggest permeability ratio was found at samples with PNIPAM concentration of 1.6 and 1.8wt%.
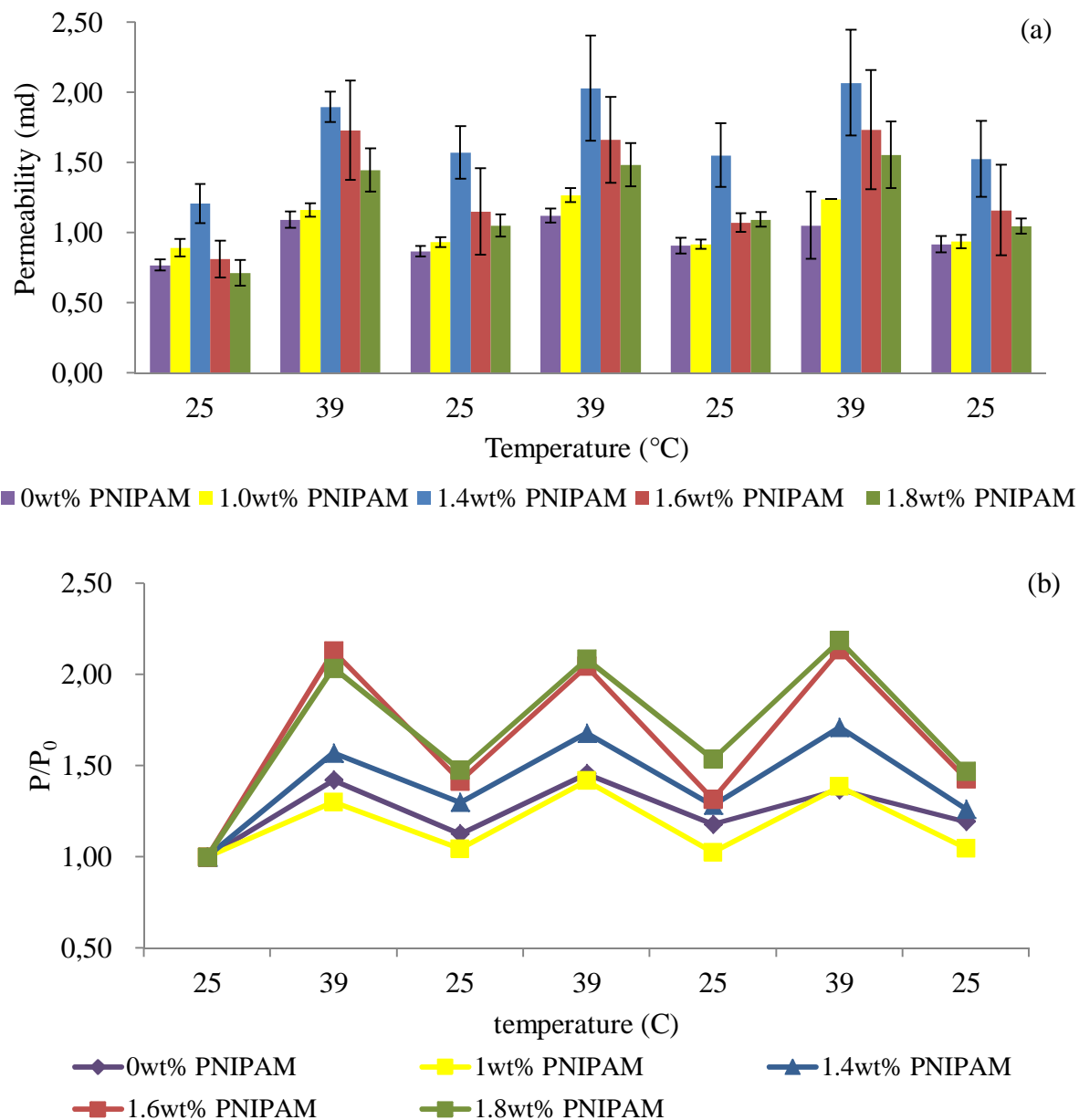
Figure 19 Liquid permeability measurements in silica–PNIPAM gels at 25 and 39°C during several temperature cycles shown as (a) permeability; (b) permeability ratio, P (permeability)/P_0 (permeability at 25°C before the first temperature change).

4.6. Diffusion measurement in silica-PNIPAM gels

4.6.1. Self-diffusion coefficient of silica-PNIPAM gels
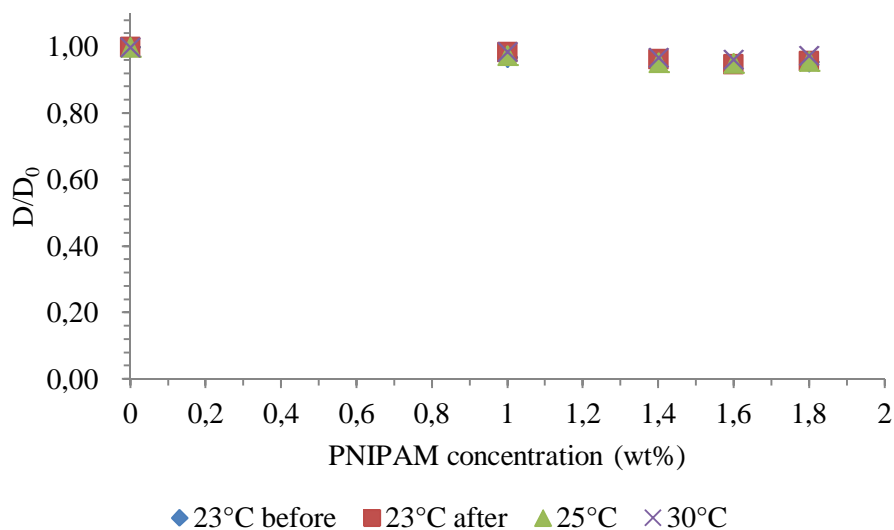
Figure 20 Relative diffusion in the silica–PNIPAM gels as measured by diffusion NMR

As shown in Figure 20, D (sample diffusion coefficient)/D_0 (pure silica diffusion coefficient) was plotted as a function of PNIPAM concentration and temperature. In contrast with flow measurement results, the relative diffusion did not change much with different PNIPAM concentrations. As expected, there was a slight increase in the diffusion coefficient with increasing temperature.

5. Discussion

The focus of this thesis is the thermal response properties of silica-PNIPAM composite gels, with the purpose of controlling liquid mass transport through the gels. The study entailed synthesis and characterization of one of the gels building blocks, PNIPAM microgels, as well as PNIPAM-co-polymer. A sol gel process was developed to formulate gels with homogenously mixed components where the microgels were mixed and gelled in a matrix of colloidal silica. The performance of the gels was evaluated on their ability to maintain structural integrity and control the mass transport of liquid through them as response to temperature changes.

5.1. PNIPAM synthesis and characterization

During synthesis of PNIPAM microgels, the reaction solution was transparent at the beginning but turned opaque shortly after ammonium persulfate was added. Both the 'melting point measurements in Figure 11 and the DLS measurements in Figure 13 indicate that the LCST of the synthesised PNIPAM particles were 32°C. The microgel size was larger than found by Hoare and colleagues [16]. They saw a change in microgel size from 700 to 200 nm when temperature increased from 25 to 40°C. The difference can probably be attributed to small differences in the synthesis procedure such as magnetic stirrer type or stirring speed. It is also possible that Hoare and colleagues did DLS measurements on redispersed lyophilized microgels. This process puts a lot of stress on the particles that might be split into smaller particles, which could explain the discrepancy between the results in this thesis and Hoare's results.

5.2. Effect of salt on colloidal silica stability

Table 1 show that the gelation time decreases with higher NaCl concentration, as the gelation time is around 24 hours and 6 minutes at a salt concentration of 0.3 and 0.9 M NaCl. As mentioned previously, the stability of a colloidal system is determined by a combination of attractive and repulsive forces. The addition of salt screens the repulsive forces [50] and in general higher salt concentration results in shorter gelation time. As previously mentioned in the results, a 0.5 M NaCl concentration provided the most suitable combination of mechanical strength and gel time (1-1.5 hours), which is why all silica-PNIPAM gels were made with this salt concentration.

5.3. Sample formulation

5.3.1. Sample formulation – silica with lyophilised PNIPAM

The reason why the lypholized PNIPAM microgels were hard to redisperse could have several reasons. According to Cheng *et al*, freeze drying can change the microstructure of PNIPAM microgels [51]. The ice crystals formed during sample freezing in the lyophilisation process sublimate leaving irregular shaped particles. Compared with spherical particles of the same size, microspheres with an irregular shape are more likely to reaggregate and or phase separate when the PNIPAM is redispersed [52, 53]. Another reason might be that the method used for lyophilisation fuses some PNIPAM microgels together so that they cannot be redispersed as they form a large connected particle network.

5.3.2. Sample formulation - silica and centrifuged PNIPAM

To avoid sample inhomogeneity, phase separation had to be avoided before sample gelation. As previously mentioned the silica concentration in the samples was set to 10 vol% while the PNIPAM concentration was varied.

The redispersion of the centrifuged PNIPAM microgels was relatively easy and the formed gels were homogenous when viewed by naked eye. As the gel with 3.27wt% PNIPAM collapsed and the gel with 2.1 wt% showed sign of collapse as response to temperature changes, it is apparent that the polymer concentration must be correct to ensure mechanically stable gels. After the collapse of the 3.27wt% PNIPAM gel, it was hypothesized that there was a strong interaction between the silica and PNIPAM so that the contracting microgels destroyed the gel network when they shrunk. Therefore experiments were made to attempt to reduce this interaction, as will be discussed just below.

In order to reduce the interaction between silica particles and PNIPAM spheres, the surfactants - Dodecyltrimethylammonium Chloride (DTAC), Hexadecyltrimethylammonium Chloride (HTAC) – was added to the system. These surfactants associate with the negatively charged silica surface [54]. This effect causes a reduction of silica surface charge and an increase of the hydrophobicity of silica because of the hydrophobic tails of the surfactant [55]. However, the gels with surfactants collapsed just as easy as without surfactants. One reason could be that the bonding between the silica particles was inhibited by the surfactant covered surface, causing unstable gels. However, it is more likely that the high microgel concentration caused the collapse.

5.4. Liquid flow through the silica-PNIPAM gels

The liquid permeability of the silica-PNIPAM gels was studied at different PNIPAM concentrations between 0-1.8 wt% PNIPAM. Figure 16 and Figure 19 show a permeability maximum at 1.4 wt% of PNIPAM. It is not surprising that the permeability is higher at relatively high microgel concentrations. According to Hoare, more thermoresponsive microgels increases the total free volume inside the gel, making higher liquid flux possible [16]. The reason for the decrease of permeability of samples with PNIPAM concentration higher than 1.4wt% could be that the microgels by themselves start to take up so much space that even though they are contracted that they start to reduce the flow through the gel.

According to Figure 16 and Figure 17, most of the particle size and permeability change takes place before the temperature reached 32°C. In 2011, Hoare observed the opposite phenomena for PNIPAM microgels containing ethyl cellulose membranes [16]. They found the microgels shrank at 30°C but showed significant increase of flux from 32°C, theorizing that the microgel volume changes at 30°C was not large enough to form sufficient free volume over the full thickness of the gel.

One possible reason for the discrepancy between this study and Hoare's report could be that the LCST of microgels has been shifted to a temperature between 30 and 32°C. There are several factors that can affect the change of LCST. The presence of for example NaCl can shift the LCST to a lower temperature [56]. Du *et al* saw that the LCST of PNIPAM was reduced to 30°C in the presence of 1M NaCl [57]. In the presence of salt, anions can polarize an adjacent water molecule that is involved in hydrogen bonding with the amide group. These species then destabilize hydrophobic hydration of the polymer and increase the surface tension which result in a decrease in the LCST [58]. The NaCl concentration in silica-PNIPAM samples was 0.5M and it is therefore possible that the LCST of the microgels was affected.

The permeability results in Figure 19 indicate that there are irreversible changes to the gel structure after the first temperature cycle. This is similar to what was found by Hoare and colleagues [16]. They saw that the permeability of the gels was lower before their material had gone through a temperature cycle. They attributed this to the time needed for water to fill the porous inside of the gel. However, in this thesis the silica-PNIPAM gels where equilibrated in water for at least one day for each data point, so water should have been fully adsorbed during the experiment, especially as the microgels expel water when they shrink, which effectively fills the pores. Another reason for the irreversible change could be that the reswelling microgels have rotated in their contracted state. If the microgel is not perfectly round as it reswells in an orientation that is different from the stating state, it might not fit perfectly in the silica matrix. This results in pores in the gels that are partly open when the microgels are swollen. This could

explain why the permeability of the gels is always higher after the first temperature cycle, than before the temperature change.

5.5. Mass transport property of silica-PNIPAM microgel by diffusion

5.5.1. 1H-NMR self-diffusion measurements

During self-diffusion coefficient experiments, there is no concentration gradient of substances or pressure differences. Water acted as the tracer molecule in the sample. Figure 20 show that there is little difference in the relative diffusion, D(gel sample)/D_0(pure silica sample), between the samples. That means that the only reason that diffusion coefficients is going up when the temperature is going up is that the water molecules moves faster, the contraction of the microgels does not matter. It seems like the diffusion through an expanded microgel, that consist of almost only water a "widely" spaced cross linked polymer strands is similar to the 'free' diffusion of water though a pore where the microgel has contracted. Therefore the water can diffuse relatively freely though the material in both states.

5.5.2. Osmotic gradient diffusion measurements

The tracer molecule for the concentration gradient diffusion measurements was methylene blue. However, the diffusion measurement could not be successfully completed. After initiating the experiment only the top part of the gel turned dark blue. Figure 21 illustrates that the blue colour did not spread down the column even though the experiment was allowed to continue for 3 weeks and almost not methylene blue was detected in the receiver chamber. Methylene blue molecules are around 1 nm in diameter [59, 60] and should for size reasons have no problem to traverse the pores of the gel in their open state as those pores have a diameter in the range of several hundreds of nm.
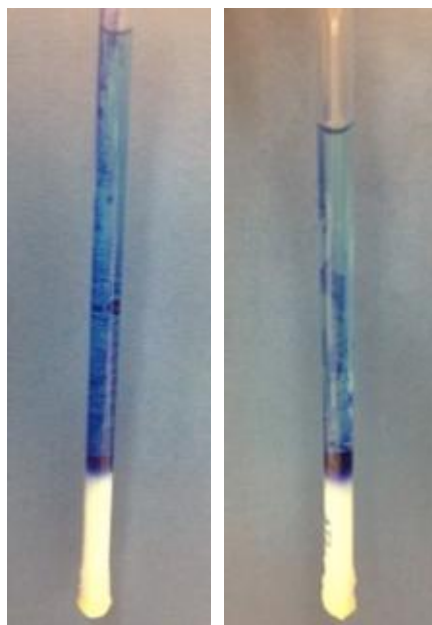
Figure 21 Methylene blue precipitations in the column used for the osmotic gradient diffusion measurement. After 1week (left) and 3 weeks (right)

It is apparent that the methylene blue precipitates on the wall of NMR tube. This might be explained by negatively charged silica surface acting as nucleating surfaces for the cationic methylene blue molecules. Over time the saturated methylene blue solution precipitated at the walls of the donor chamber and in the gel [61]. The precipitation in the gels might have blocked the pores of the gels, hindering diffusion of methylene blue through the gel.

6. Conclusion

A new type of silica-PNIPAM composite has been formulated that can mechanically withstand temperature cycling and a moderate water induced pressure gradients without breaking.

The permeability of water though the gels can be regulated by changing the temperature and PNIPAM concentration and a maximum in the permeability was found at a PNIPAM concentration of 1.4 wt%. In samples with PNIPAM a reversible change in permeability could be achieved during cyclically temperature changes.

However, the relative diffusion (D/D_0) over the gels when there was no pressure difference was not affected by temperature variations. It is hypothesised that water diffusion is roughly equally hindered in pores filled with expanded or contracted PNIPAM microgels. The osmotic gradient diffusion measurement failed because of lacking diffusive mobility of the methylene blue molecule in the used set up. Instead another type of tracer molecule should be used that interacts

less with the charged silica surfaces under the used conditions, for example Congo red or acid fuchsine.

The silica-PNIPAM composite material could be used for controlled release in material science and biotechnology applications. Moreover, the mass transport findings in this thesis are of general importance for materials and suspensions containing soft materials as they highlight differences between diffusion and flow through the pores of these materials.

7. Acknowledgement

I would like to express my deepest appreciation to Christoffer Abrahamsson, the main supervisor of this thesis, who patiently gave me a lot of guidance, encouragement and advises, as well as the NMR self-diffusion results. To Mikael Larsson, for his support and advises as a supervisor during the time I was in Ian Wark Research Institute. I would like to thank Michael Persson, the examiner of this thesis, and Magnus Nydén, director of Ian Wark Research Institute, for valuable advices. In addition, a thank you to all the co-workers in division of Applied Surface Chemistry, thank you for sharing your experience and creating such an awesome atmosphere. Finally, I would like to thank my parents for their support and unconditional love during this work.

Reference

1. Fan, L.-t. and S.K. Singh, *Controlled release: A quantitative treatment.* 1989: Springer-Verlag Berlin.

2. Risbud, M.V., et al., *pH-sensitive freeze-dried chitosan–polyvinyl pyrrolidone hydrogels as controlled release system for antibiotic delivery.* Journal of controlled release, 2000. 68(1): p. 23-30.

3. Starodoubtsev, S.G., et al., *Evidence for polyelectrolyte/ionomer behavior in the collapse of polycationic gels.* Macromolecules, 1995. 28(11): p. 3930-3936.

4. Okore, V.C., *Effect of dika fat content of a barrier film coating on the kinetics of drug release from swelling polymeric systems.* Bollettino chimico farmaceutico, 2000. 139(1): p. 21.

5. Uhrich, K.E., et al., *Polymeric systems for controlled drug release.* Chemical reviews, 1999. 99(11): p. 3181-3198.

6. Otsuka, H., Y. Nagasaki, and K. Kataoka, *PEGylated nanoparticles for biological and pharmaceutical applications.* Advanced Drug Delivery Reviews, 2003. 55(3): p. 403-419.

7. Pelton, R., *Poly (N-isopropylacrylamide)(PNIPAM) is never hydrophobic.* Journal of colloid and interface science, 2010. 348(2): p. 673-674.

8. Lin, C.-C. and A.T. Metters, *Hydrogels in controlled release formulations: network design and mathematical modeling.* Advanced drug delivery reviews, 2006. 58(12): p. 1379-1408.

9. Stella, V.J. and K.J. Himmelstein, *Prodrugs and site-specific drug delivery.* Journal of medicinal chemistry, 1980. 23(12): p. 1275-1282.

10. Heller, J., *Controlled release of biologically active compounds from bioerodible polymers.* Biomaterials, 1980. 1(1): p. 51-57.

11. Qiu, Y. and K. Park, *Environment-sensitive hydrogels for drug delivery.* Advanced drug delivery reviews, 2001. 53(3): p. 321-339.

12. Siegel, R.A., et al., *pH-controlled release from hydrophobic/polyelectrolyte copolymer hydrogels.* Journal of controlled release, 1988. 8(2): p. 179-182.

13. You, Y.-Z., K.K. Kalebaila, and S.L. Brock, *Temperature-controlled uptake and release in PNIPAM-modified porous silica nanoparticles.* Chemistry of Materials, 2008. 20(10): p. 3354-3359.

14. Baker, R.W., *Controlled release delivery system by an osmotic bursting mechanism.* 1976, Google Patents.

15. Miyazaki, S., C. Yokouchi, and M. Takada, *External control of drug release: controlled release of insulin from a hydrophilic polymer implant by ultrasound irradiation in diabetic rats.* Journal of Pharmacy and Pharmacology, 1988. 40(10): p. 716-717.

16. Hoare, T., et al., *Magnetically triggered nanocomposite membranes: a versatile platform for triggered drug release.* Nano letters, 2011. 11(3): p. 1395-1400.

17. Santini, J.T., M.J. Cima, and R. Langer, *A controlled-release microchip.* Nature, 1999. 397(6717): p. 335-338.

18. ZacháHilt, J., *Hydrogel nanocomposites: a review of applications as remote controlled biomaterials.* Soft Matter, 2010. 6(11): p. 2364-2371.

19. Griffin, D.R., J.T. Patterson, and A.M. Kasko, *Photodegradation as a Mechanism for Controlled Drug Delivery.* Biotechnology and Bioengineering, 2010. 107(6): p. 1012-1019.

20. Kobayashi, K. and H. Suzuki, *A sampling mechanism employing the phase transition of a gel and its application to a micro analysis system imitating a mosquito.* Sensors and Actuators B: Chemical, 2001. 80(1): p. 1-8.

21. Chu, L.Y., et al., *Thermoresponsive transport through porous membranes with grafted PNIPAM gates.* AIChE Journal, 2003. 49(4): p. 896-909.

22. Suzuki, H., *Stimulus-responsive gels: Promising materials for the construction of micro actuators and sensors.* Journal of intelligent material systems and structures, 2006. 17(12): p. 1091-1097.

23. Achmetov, B.V., et al., *Physical and colloid chemistry.* 1989: Mir Publ.

24. William, F.S. and J. Hashemi, *Foundations of materials science and engineering.* 2006: Mcgraw-Hill Publishing.

25. Jones, K.R., *On the differential form of Darcy's law.* Journal of Geophysical Research, 1962. 67(2): p. 731-732.

26. Bergna, H.E. and W.O. Roberts, *Colloidal silica: fundamentals and applications.* 2005: CRC Press.

27. Bergenståhl, B.A. and J. Alander, *Lipids and colloidal stability.* Current opinion in colloid & interface science, 1997. 2(6): p. 590-595.

28. Ishikawa, Y., Y. Katoh, and H. Ohshima, *Colloidal stability of aqueous polymeric dispersions: effect of pH and salt concentration.* Colloids and Surfaces B: Biointerfaces, 2005. 42(1): p. 53-58.

29. Tiller, C.L. and C.R. O'Melia, *Natural organic matter and colloidal stability: Models and measurements.* Colloids and Surfaces A: Physicochemical and Engineering Aspects, 1993. 73: p. 89-102.

30. Wiese, G. and T. Healy, *Effect of particle size on colloid stability.* Trans. Faraday Soc., 1970. 66: p. 490-499.

31. Yotsumoto, H. and R.-H. Yoon, *Application of extended DLVO theory: I. Stability of rutile suspensions.* Journal of colloid and interface science, 1993. 157(2): p. 426-433.

32. Grahame, D.C., *The electrical double layer and the theory of electrocapillarity.* Chemical Reviews, 1947. 41(3): p. 441-501.

33. Skipper, N., et al., *Direct measurement of the electric double-layer structure in hydrated lithium vermiculite clays by neutron diffraction.* The Journal of Physical Chemistry, 1995. 99(39): p. 14201-14204.

34. Guldbrand, L., et al., *Electrical double layer forces. A Monte Carlo study.* The Journal of chemical physics, 1984. 80(5): p. 2221-2228.

35. Liese, A. and L. Hilterhaus, *Evaluation of immobilized enzymes for industrial applications.* Chemical Society Reviews, 2013. 42(15): p. 6236-6249.

36. Marqusee, J. and J. Ross, *Kinetics of phase transitions: Theory of Ostwald ripening.* The Journal of chemical physics, 1983. 79(1): p. 373-378.

37. Hench, L.L. and J.K. West, *The sol-gel process.* Chemical Reviews, 1990. 90(1): p. 33-72.

38. Voorhees, P.W., *The theory of Ostwald ripening.* Journal of Statistical Physics, 1985. 38(1-2): p. 231-252.

39. Allen, L.H. and E. Matijević, *Stability of colloidal silica: I. Effect of simple electrolytes.* Journal of colloid and interface science, 1969. 31(3): p. 287-296.

40. Iler, R.K., *The chemistry of silica: solubility, polymerization, colloid and surface pro perties, and biochemistry.* 1979: Wiley.

41. Dan, L., et al., *Intelligent Cell Detachment Materials Based on Poly (N-Isopropylacrylamide).* Progress in Chemistry, 2011. 23(11): p. 2353-2359.

42. Morris, G.E., B. Vincent, and M.J. Snowden, *Adsorption of Lead Ions onto< i> N</i>-Isopropylacrylamide and Acrylic Acid Copolymer Microgels.* Journal of colloid and interface science, 1997. 190(1): p. 198-205.

43. Cheng, X., et al., *Surface chemical and mechanical properties of plasma-polymerized N-isopropylacrylamide.* Langmuir, 2005. 21(17): p. 7833-7841.

44. Kujawa, P., et al., *Temperature-sensitive properties of poly (N-isopropylacrylamide) mesoglobules formed in dilute aqueous solutions heated above their demixing point.* Macromolecules, 2006. 39(22): p. 7686-7693.

45. Dong, L.-C. and A.S. Hoffman, *Synthesis and application of thermally reversible heterogels for drug delivery.* Journal of Controlled Release, 1990. 13(1): p. 21-31.

46. Boutris, C., E. Chatzi, and C. Kiparissides, *Characterization of the LCST behaviour of aqueous poly (N-isopropylacrylamide) solutions by thermal and cloud point techniques.* Polymer, 1997. 38(10): p. 2567-2570.

47. Schmidt, S., T. Hellweg, and R. von Klitzing, *Packing density control in P (NIPAM-co-AAc) microgel monolayers: effect of surface charge, pH, and preparation technique.* Langmuir, 2008. 24(21): p. 12595-12602.

48. Abrahamsson, C., et al., *Magnetically induced structural anisotropy in binary colloidal gels and its effect on diffusion and pressure driven permeability.* Soft matter, 2014. 10(24): p. 4403-4412.

49. Hoare, T.R., et al., *Magnetic heating for drug delivery and other applications.* 2009, Google Patents.

50. Trompette, J.L. and M. Meireles, *Ion-specific effect on the gelation kinetics of concentrated colloidal silica suspensions.* Journal of colloid and interface science, 2003. 263(2): p. 522-527.

51. Cheng, C.-J., et al., *Effect of freeze-drying and rehydrating treatment on the thermo-responsive characteristics of poly (N-isopropylacrylamide) microspheres.* Colloid and Polymer Science, 2008. 286(5): p. 571-577.

52. Mosharraf, M. and C. Nyström, *The effect of particle size and shape on the surface specific dissolution rate of microsized practically insoluble drugs.* International Journal of Pharmaceutics, 1995. 122(1): p. 35-47.

53. Zhanpeng, J. and G. Yuntao, *Flocculation morphology: effect of particulate shape and coagulant species on flocculation.* Water Science & Technology, 2006. 53(7): p. 9-16.

54. Huang, Z., Z. Yan, and T. Gu, *Mixed adsorption of cationic and anionic surfactants from aqueous solution on silica gel.* Colloids and surfaces, 1989. 36(3): p. 353-358.

55. Koopal, L.K., et al., *The effect of cationic surfactants on wetting, colloid stability and flotation of silica.* Colloids and Surfaces A: Physicochemical and Engineering Aspects, 1999. 151(1): p. 15-25.

56. Liu, X., et al., *Unusual salt effect on the lower critical solution temperature of hyperbranched thermoresponsive polymers.* Soft Matter, 2008. 4(10): p. 1991-1994.

57.   Du, H., R. Wickramasinghe, and X. Qian, *Effects of salt on the lower critical solution temperature of poly (N-isopropylacrylamide).* The Journal of Physical Chemistry B, 2010. 114(49): p. 16594-16604.

58.   Zhang, Y., et al., *Specific ion effects on the water solubility of macromolecules: PNIPAM and the Hofmeister series.* Journal of the American Chemical Society, 2005. 127(41): p. 14505-14510.

59.   Hang, P.T. and G.W. Brindley, *Methylene blue absorption by clay minerals. Determination of surface areas and cation exchange capacities (clay-organic studies XVIII).* Clays and clay minerals, 1970. 18(4): p. 203-212.

60.   Wang, S., et al., *The physical and surface chemical characteristics of activated carbons and the adsorption of methylene blue from wastewater.* Journal of Colloid and Interface Science, 2005. 284(2): p. 440-446.

61.   Bujdák, J. and P. Komadel, *Interaction of methylene blue with reduced charge montmorillonite.* The Journal of Physical Chemistry B, 1997. 101(44): p. 9065-9068.